Combining biorelevant *in vitro* and *in silico* tools to investigate the *in vivo* performance of the amorphous solid dispersion formulation of etravirine in the fed state..

Chara Litou[1], David B. Turner[2], Nico Holmstock[3], Jens Ceulemans[3], Karl J. Box[4], Edmund Kostewicz[1], Martin Kuentz[5], Rene Holm[3], Jennifer Dressman[1,6*]

[1]Institute of Pharmaceutical Technology, Goethe University, Frankfurt am Main, Germany

[2]Certara UK Limited, Simcyp Division, Level 2-Acero, 1 Concourse Way, Sheffield, S1 2BJ, UK

[3]Drug Product Development, Janssen R&D, Johnson & Johnson, Turnhoutseweg 30, 2340 Beerse, Belgium

[4]University of Applied Sciences and Arts Northwestern Switzerland, Hofackerstr. 30, 4132, Switzerland

[5]Pion Inc. (UK) Ltd., Forest Row, East Sussex, UK

[6]Fraunhofer Institute of Translational Pharmacology and Medicine, Frankfurt, Germany

Running Title: PBPK modeling evaluation of an amorphous solid dispersion of etravirine

*To whom correspondence should be addressed:

Prof. Dr. Jennifer Dressman, Institute of Pharmaceutical Technology, Biocenter, Johann Wolfgang Goethe University, Max-von-Laue-Str. 9, 60438 Frankfurt am Main, Germany.

E-mail: dressman@em.uni-frankfurt.de

ABSTRACT

Introduction: In the development of bio-enabling formulations, innovative *in vivo* predictive tools to understand and predict the *in vivo* performance of such formulations are needed. Etravirine, a non-nucleoside reverse transcriptase inhibitor, is currently marketed as an amorphous solid dispersion (Intelence® tablets). The aims of this study were 1) to investigate and discuss the advantages of using biorelevant *in vitro* setups in simulating the *in vivo* performance of Intelence® 100 mg and 200 mg tablets, in the fed state, 2) to build a Physiologically Based Pharmacokinetic (PBPK) model by combining experimental data and literature information with the commercially available *in silico* software Simcyp® Simulator V17.1 (Certara UK Ltd.), and 3) to discuss the challenges when predicting the *in vivo* performance of an amorphous solid dispersion and identify the parameters which influence the pharmacokinetics of etravirine most.

Methods: Solubility, dissolution and transfer experiments were performed in various biorelevant media simulating the fasted and fed state environment in the gastrointestinal tract. An *in silico* PBPK model for healthy volunteers was developed in the Simcyp® Simulator, using *in vitro* results and data available from the literature as input. The impact of pre- and post-absorptive parameters on the pharmacokinetics of etravirine was investigated using simulations of various scenarios.

Results: *In vitro* experiments indicated a large effect of naturally occurring solubilizing agents on the solubility of etravirine. Interestingly, supersaturated concentrations of etravirine were observed over the entire duration of dissolution experiments on Intelence® tablets. Coupling the *in vitro* results with the PBPK model provided the opportunity to investigate two possible absorption scenarios, i.e. with or without implementation of precipitation. The results from the simulations suggested that a scenario in which etravirine does not precipitate is more representative of the *in vivo* data. On the post-absorptive

side, it appears that the concentration dependency of the unbound fraction of etravirine in plasma has a significant effect on etravirine pharmacokinetics.

Conclusions: The present study underlines the importance of combining *in vitro* and *in silico* biopharmaceutical tools to advance our knowledge in the field of bio-enabling formulations. Future studies on other bio-enabling formulations can be used to further explore this approach to support rational formulation design as well as robust prediction of clinical outcomes.

KEYWORDS

PBPK, modeling and simulation, amorphous solid dispersions, bio-enabling formulations, etravirine

1. Introduction

Various innovative formulation approaches have emerged in recent years in order to address the increasingly challenging physicochemical properties of new Active Pharmaceutical Ingredients (APIs). Inadequate solubility and/or dissolution rate often limit the rate and extent of absorption of such APIs after oral administration. Bio-enabling formulation strategies, such as nano-formulations, complexation with cyclodextrins, amorphous dispersions and self-emulsifying drug delivery systems, are nowadays utilized in drug development pipelines with the goal of increasing bioavailability.[1,2] However, the *in vitro* characterization of the *in vivo* behavior of these formulations could still benefit from an approach providing more fundamental mechanistic insight.[2,3]

One of the goals of the European Research Program "PEARRL" (www.pearrl.eu) is to design and deliver tools which will enable a better understanding of the *in vivo* performance of bio-enabling formulations. Within the framework of the PEARRL consortium (and as a follow-up to a recently published case example)[4], the present study aims to combine results obtained with biorelevant *in vitro* tools with *in silico* modeling techniques to simulate and better understand the *in vivo* behavior of the amorphous solid dispersion of etravirine. This formulation of etravirine is commercially available under the brand name Intelence® and its labeling specifies administration in the fed state.

Etravirine is a second generation non-nucleoside reverse transcriptase inhibitor used for the treatment of HIV-1 infection in treatment-experienced adult patients and pediatric patients two years of age and older, usually in combination with other anti-retroviral agents.[5–7] It has been classified as a BCS Class IV compound as it has very low aqueous solubility, irrespective of the pH (solubility in water is reported to be lower than 1 µg/mL)[8], and low to intermediate permeability.[9] It is a weakly basic compound (reported pKa values are 4.5, 3.75 and <3)[10–12] with a high logP value (reported values are 5.2 and 5.54)[10,13]. In the literature there have only been a few attempts thus far to characterize etravirine *in vitro*. Bevernage et al. measured the solubility of crystalline etravirine in various versions of biorelevant

media, as well as in pooled human gastric and intestinal aspirates. The measured solubility values at 24 h were 0.061, 1.48 and 4.05 µg/mL in pooled fasted human gastric fluids ("FaHGF"), pooled fasted human intestinal fluids ("FaHIF") and pooled fed human intestinal fluids (obtained after the administration of 400 mL of Ensure Plus®, "FeHIF"), respectively.[10,14]

To overcome the poor physicochemical properties of crystalline etravirine and to improve its bioavailability, the manufacturer attempted a variety of different enabling technologies. However, most of them did not result in advantageous outcomes (for example, an orally dosed nano-suspension resulted in negligible plasma concentrations in dogs)[8]. Among the various formulations developed and administered in different phases of the clinical trials, the amorphous solid dispersion of etravirine was the most promising formulation, and is nowadays the commercial formulation (Intelence®).[8,9] In particular, according to the EMA Public Assessment Report, the formulations used in the clinical studies were as follows: 1) TF002: PEG-4000-based capsule, early Phase I and IIa studies, 2) TF035: HPMC tablet using granulo-layering technology, late Phase I and II studies, 3) F060: HPMC tablet using spray-drying technology, pivotal Phase III studies (commercial formulation).[9]

Despite the extensive clinical study program conducted and the various bridging bioequivalence studies between the different formulations, the pharmacokinetics and *in vivo* behavior of etravirine have not yet been fully explained.[7,9] For example, in Study C141 a single dose of 100 mg of the commercial formulation (F060) was found to be bioequivalent to a single dose of 800 mg of the exploratory formulation TF035, but in Study C228 bioequivalence could not be confirmed between the 100 mg of F060 and 800 mg of TF035 after multiple dosing for 7 days b.i.d. Additionally, multiple-dose administration of F060 at a dose of 200 mg resulted in an etravirine exposure that was approximately 70% higher than that obtained with the 800 mg multiple-dose administration of the TF035.[9]

98 The recommended dose of Intelence® for adults is 100 mg or 200 mg, taken orally twice daily following
99 a meal.[6,7] The bioavailability of Intelence® in the fed state is increased by up to 50% in comparison to
100 the bioavailability in the fasted state.[7,9,12] Moreover, the pharmacokinetics of Intelence® seem to be
101 more than dose proportional. However, the absolute bioavailability has not been determined since no
102 intravenous formulation is available.

103 The aims of this study were threefold: 1) to investigate the advantages of using biorelevant *in vitro* setups
104 in simulating the *in vivo* performance of Intelence® in the fed state, 2) to build a physiologically based
105 pharmacokinetic (PBPK) model for etravirine in the fed state by combining experimental data and
106 literature information with the commercially available *in silico* software Simcyp® Simulator V17.1 (Certara
107 UK Ltd.), and 3) to assess the importance of pre- and post-absorptive aspects in determining the
108 pharmacokinetic response to administration of the amorphous solid dispersion of etravirine.

109

2. Materials and Methods

2.1 Chemicals and reagents

Etravirine powder was kindly donated by Janssen, Belgium. Acetonitrile and water of HPLC grade were obtained from Merck KGaA (Darmstadt, Germany). Sodium dihydrogen phosphate dehydrate of analytical grade was from Merck KGaA (Darmstadt, Germany). Phosphoric acid, sodium chloride and sodium hydroxide were of analytical grade and purchased from VWR chemicals (Leuven, Belgium). Intelence® tablets were commercially purchased from a German pharmacy (Lot # and PZN were HKL1Q00, 06733695 for the 100 mg and IEL3Y00, 08894758 for the 200 mg strength, respectively). Pepsin was purchased from Sigma-Aldrich (Lot # SLBQ2263V). Lipofundin® MCT/LCT 20% was purchased from BRAUN (B. Braun Melsungen AG, Melsungen, Germany). Fasted state simulated gastric fluid (FaSSGF)/fasted state simulated intestinal fluid (FaSSIF V1)/fed state simulated intestinal fluid (FeSSIF V1) powder (lot 01-1512-05NP), FeSSIF V2 powder (lot 03-1610-02) and FaSSIF V3 powder (lot PHA S 1306023) were kindly donated by Biorelevant.com Ltd., (Surrey, UK).

2.2 Experimental Methods

2.2.1 Solubility experiments

The solubility of crystalline etravirine was investigated in various Level I and Level II biorelevant media,[15,16] using the Uniprep™ system (Whatman®, Piscataway, NJ, USA), as previously described by Andreas et al.[17] Briefly, an excess amount of etravirine was added to a 3 mL aliquot of the medium and the samples were shaken for 2, 4, 8 and 24 h at 37 °C on an orbital mixer. In agreement with literature data for etravirine, equilibrium was reached by 24 h.[18] After shaking, the samples were immediately filtered through pre-warmed 0.45 µm PTFE filters and analyzed by HPLC. Solubility measurements were carried out at least in triplicate ($n \geq 3$) and the final pH of the medium (pH_{final}) was recorded in all cases. In every case the pH_{final} was only slightly or not at all different from the initial pH value of the medium.

2.2.2 Dissolution experiments

Dissolution experiments of the Intelence® tablets were performed using the paddle (USP II) apparatus (Erweka DT 600, Heusenstamm, Germany). Each vessel contained 250 mL for media simulating gastric fluids and 500 mL when simulating intestinal fluids. The rotating speed of the paddle was set at 75 rpm. The temperature in the vessels was maintained at 37.0 ± 0.5 °C throughout the experiment. Samples were withdrawn at 5, 7.5, 10, 15, 20, 30, 40, 60, 90, 120, 150, 180, 210, 240 and 1440 min with glass syringes, through a cylindrical polyethylene filter stick with a pore size of 4 µm attached to the end of the sampling tubes. Immediately thereafter, the samples were filtered through 0.45 µm PTFE filters (Whatman®, Piscataway, NJ, USA). After discarding the first 1 mL, the filtrate was diluted with mobile phase and analyzed by HPLC. All dissolution experiments were performed in triplicate (n=3) and the final pH in the vessels was recorded in all cases. At the end of the 24 h dissolution experiment, any solid remaining in the dissolution vessel was collected, separated from the liquid medium, dried in a vacuum drying oven (Heraeus VTR 5022, Heraeus Holding GmbH, Hanau, Germany) and analysed by Differential Scanning Calorimetry (DSC 6000 with Autosampler, Perkin Elmer, Waltham, USA).

2.2.3 Transfer experiments

Transfer experiments were performed for both the 100 mg and 200 mg Intelence® capsules utilizing the USP II apparatus, as described previously by Berlin et al.[19] Briefly, 250 mL of Level III FaSSGF pH 2.0 and 350 mL of Level II FaSSIF V1, FaSSIF V3, or FaSSIF $V1_{concentrated}$ (5.14 mM NaTC, in order to account for the dilution occurring after transfer) were used as the dissolution media in the gastric and duodenal compartments, respectively. The rotating speed of the paddles was set at 75 rpm. The temperature in the vessels was maintained at 37.0 ± 0.5 °C throughout the experiment. A peristaltic pump set to first order kinetics ($t_{1/2}$ = 9 min) was used to transfer the medium from the gastric to the duodenal compartment, from which samples were withdrawn at 5, 10, 15, 20, 30, 45, 60, 75, 90, 120, 180 and 240 min. Sample handling and analysis were as described for the dissolution experiments.

2.2.4 Chromatographic assays

For the quantitative analysis of the samples, a HPLC-UV system was used (Hitachi Chromaster; Hitachi Ltd., Tokyo, Japan or Spectra System HPLC, ThermoQuest Inc., San Jose, USA). The analytical column was a BDS Hypersil C18, 3 μm, 150 x 3 mm (Thermo Scientific) combined with a pre-column (BDS Hypersil C-18, 3 μm, 10 x 4 mm). The mobile phase consisted of 60:40 % v/v AcN : H_2O. The detection wavelength was set at 310 nm, the injection volume at 20 μL and the flow rate at 0.8 mL/min. The limit of detection (LOD) and of quantification (LOQ) were 0.01 μg/mL and 0.05 μg/mL, respectively.

2.3 Pharmacokinetic data and methods

2.3.1 *In vivo* studies

Data from five clinical studies with the commercial formulation (F060) were used to support the development and verification of the PBPK model of etravirine. In all cases, etravirine was administered orally, since no intravenous formulation is available.[9]

The first study was an open-label, randomized, crossover study conducted in 37 healthy volunteers (29% females). The subjects were administered one 100 mg Intelence® (non-coated) tablet, four 25 mg non-coated etravirine tablets, or one 100 mg etravirine tablet dispersed in 100 mL water, along with approximately 200 mL of water and a standardized breakfast.[20]

The second study was an open-label, randomized, crossover study, conducted in 24 healthy volunteers (25% females), with the aim of comparing the bioavailability of etravirine administered as one 200 mg Intelence® tablet, or as two 100 mg Intelence® tablets. In this study, the subjects were administered a) two 100 mg Intelence® tablets, b) one 200 mg Intelence® tablet, in both cases after the administration of a standard breakfast, c) two 100 mg coated etravirine tablets, or d) one 200 mg coated etravirine tablet.[20]

The third study was an open-label, randomized, crossover study, conducted in 24 healthy male volunteers with the aim of investigating the effect of various meals on the bioavailability of etravirine. The subjects were administered one 100 mg Intelence® tablet along with approximately 200 mL of water and one of the following meals: a) standard, b) light, c) enhanced fiber or d) high-fat breakfast. A standard lunch was served 4.5 hours after dosing.[12]

The fourth study was an open-label, randomized, crossover study, conducted in 18 healthy volunteers (58% females). The subjects were administered a 100 mg Intelence® tablet alone, along with 200 mL of water and a standardized breakfast, or with a) 150 mg ranitidine b.i.d. for eleven days, or b) 40 mg of omeprazole q.d. for eleven days.[21]

The fifth study aimed to investigate the pharmacokinetics of etravirine in HIV-patients with mild and moderate hepatic impairment (% female not reported), in comparison to their matched healthy control volunteers (n=8). The subjects were administered a 200 mg Intelence® tablet twice daily along with 200 mL of water and a standardized breakfast/lunch, on study days 1 to 7.[22] Only the pharmacokinetic profiles of Day 1 of the healthy matched controls were used for the purposes of the current study.

For the first two clinical studies, individual pharmacokinetic data were available (kindly provided by Janssen, Belgium - data on file)[20], whereas for the later three clinical studies, only mean (without standard deviations) pharmacokinetic profiles were available, which were derived and digitalized from the respective studies[12,21,22] using the WebPlotDigitizer (version 4.1; PLOTCON; Oakland, USA). All available demographic data from the aforementioned clinical studies were used in the simulations of the clinical trials.

2.3.2 Etravirine pharmacokinetic parameters obtained from the literature

Etravirine is extensively bound to plasma proteins (approximately 99%, albumin and α1-acid glycoprotein) and the reported average blood to plasma concentration ratio in humans is 0.7, although

intersubject variation is high.[9] A detailed study in which the metabolism of etravirine was evaluated using human liver microsomes, cDNA expressed cytochromes P450s and UDP-glucuronosyltransferases has been published by Yanakakis and Bumpus.[23] Etravirine is mainly metabolized by CYP3A4 and CYP2C19, although CYP2C9 and UGT 1A3 and 1A8 are also involved. Seven metabolites were identified in total by Yanakakis and Bumpus, however, K_m and V_{max} values were provided only for four out of the seven.[23] By contrast, the renal clearance of etravirine is minimal. The mean plasma half-life is reported to be approximately 41 h and ranges from 21 h to 61 h.[24] Etravirine also exhibits large inter- (approximately 80%) and intra-individual (approximately 40%) variability in other pharmacokinetic parameters. Even taking this variability into account, the pharmacokinetics of this compound appear to be more than dose proportional.[9] It has additionally been noted that etravirine exposure appears to be lower in HIV-1 infected patients than in healthy subjects.[9]

In the literature there have only been a few attempts to explain the *in vivo* behavior of this compound using *in silico* approaches. Of these, most have focused on the metabolism of the drug and potential Drug-Drug Interactions (DDIs) in population pharmacokinetic studies conducted in HIV-1 infected patients.[25–28] Despite efforts to explain the observed variability in the elimination of etravirine, no robust conclusions could be reached and only a small percentage of the variability could be explained. In all the aforementioned studies, body weight was identified as an important parameter affecting the PK of etravirine, however, no specific data were made available regarding body composition of the enrolled subjects.

Green et al.[26] and Lubomirov et al.[27] attempted to identify the impact of CYP2C9/CYP2C19 phenotype on the pharmacokinetics of etravirine. Despite the fact that variations in the CYP2C9/CYP2C19 phenotype (i.e. extensive, intermediate, poor metabolizer) had an effect on the metabolism of etravirine, only 5-16% of the overall variability in the apparent clearance of etravirine could be explained by the genetic differences, indicating that other factors must be involved in the elimination of etravirine.

Last, but not least, it is interesting to note the wide range of apparent volume of distribution for etravirine reported in the respective population-pharmacokinetic studies i.e. 420-1370 L,[13,26–29] again suggesting that etravirine is a compound with a challenging post-absorptive behavior.

2.3.3 Modeling methods and strategies

PBPK modeling and simulations were performed using the Simcyp® Simulator (V17.1; Certara, Sheffield, UK). All relevant input parameters for the development of the PBPK models and simulations are summarized in Table 1.

Based on the properties of the compound as well as the apparent volumes of distribution (420-1370 L)[13,26–29] reported in the literature, a full PBPK model was set up for etravirine. The apparent volume of distribution and clearance were estimated using the Parameter Estimation (PE) Tool, by simultaneously fitting these parameters to all individual PK profiles available for the 100 mg and 200 mg dose strength. In particular, the apparent volume of distribution was estimated based on the Rodgers-Rowland equation and was kept constant at both doses (i.e. same apparent volume of distribution for 100 mg and 200 mg dose strength). For the enzyme kinetics the values reported in the study of Yanakakis and Bumpus[23] were used, as previously described in population PK studies in the literature [25,26], whereas the clearance due to other pathways was estimated from the available individual *in vivo* profiles for the 100 mg and 200 mg doses under the assumption of a constant apparent volume of distribution at both doses. Since etravirine pharmacokinetics are not dose-proportional, the clearance estimated for the additional pathways was different for each dose, such that for the 200 mg dose the value was approximately half of the value estimated for the 100 mg dose. It should be noted that despite all efforts, only approximately 20% of the clearance can be accounted for in a mechanistic way in the current adult PBPK model and further efforts are required to elucidate the mechanisms involved.

To model the absorption process, the Advanced Dissolution, Absorption and Metabolism (ADAM) model was utilized. This model divides the gastrointestinal tract to 9 anatomically distinct segments starting

from stomach through small intestine to the colon, and has been described in detail by Jamei et al. and Darwich et al.[30,31] The apparent permeability of etravirine was set at 6.5 x 10^{-6} cm/s, as reported in a Caco2 assay (but, with no accompanying permeability values for reference compounds, Janssen data on file).

One of the challenges that must often be faced when attempting to build a detailed solubility/dissolution model for bio-enabling formulations based on *in vitro* data is that the properties of the drug may have been deliberately altered in the formulation vis à vis those of the unformulated drug. In this case etravirine is presented in the amorphous form in the commercial formulation, whereas the pure drug is crystalline. Based on the *in vitro* results obtained in the current study (see Results section) and with a view to simulating the absorption and explaining the *in vivo* behavior of etravirine, two approaches were followed: a) in the first approach the maximum observed concentration dissolved for each dose is used as the "solubility" of the amorphous/formulated drug. This approach assumes that etravirine would not precipitate *in vivo*, due to absorption of the API and/or its dilution in the intestinal fluids and will subsequently be referred to as the "no-precipitation approach" and b) in the second approach the concentration achieved in the dissolution vessel after 24 h is used as the "solubility" of the amorphous/formulated drug. In this approach, observed supersaturation ratios and precipitation rate constants are implemented. These are calculated by comparing the maximum observed concentration dissolved in the individual dissolution vessel with the 24 hour concentration in the same vessel and measuring the time needed to reach the "solubility" value (concentration after 24 hours). This approach will subsequently be referred to as the "implementation of precipitation" approach.

Table 1: Parameter values used for the simulations of the in vivo performance of Intelence® in the fed state

Parameter	Value	Reference/ Comments
Physicochemical & Blood Binding		
MW (g/mol)	453.28	
$logP_{o:w}$	5.2	Janssen data on file

pKa	3.5	Janssen data on file
Blood/ Plasma ratio	0.7	[7,9]
Fraction unbound in plasma	0.01	[9,11,25]
Absorption		
Model	ADAM	
$P_{app, Caco2}$ ($x10^{-6}$ cm/s)	6.5	Janssen data on file
Formulation type	Immediate release	Commercial labeling
Solubility-Diffusion Layer Model		
	No precipitation approach	
Total solubility in segment		
For 100 mg dose (µg/mL)	140, 143	Stomach, Small Intestine
For 200 mg dose (µg/mL)	310, 170	Stomach, Small Intestine
	Implementation of precipitation approach	
Total solubility in segment		
For both 100 mg and 200 mg (µg/mL)	29.4, 23.9	Stomach, Small Intestine
Kinetic Solubility (Model 1)		
Critical Supersaturation Ratio	6, 8	100 mg, 200 mg
Precipitation Rate Constant (1/h)	0.31, 0.41	100 mg, 200 mg
Distribution		
Model	Full PBPK	
V_{ss} (L/kg)	5.36	PE Tool, Method 2
Elimination		
Elimination Type	Enzyme Kinetics	
V_{max} (pmol/mg/min)	0.072, 0.067, 5.57, 0.166	For CYP3A4-M1, CYP3A4-M2, CYP2C19 and CYP3A4-M3, respectively[23]
K_m (µM)	5.83, 72.85, 7.33, 27.8	
f_{umic}	0.0935	Simcyp Prediction Toolbox
Additional clearance-HLM (µL/min/mg protein)	900, 400	PE Tool for 100 mg, 200 mg
Renal clearance (L/h)	0.0006	

271

272 *2.4 Data analysis and statistics*

273 The data derived from solubility, dissolution and transfer experiments are presented as the arithmetic

274 means with standard deviations. All PK profiles obtained from the literature were digitalized with the

WebPlotDigitizer (version 4.1; PLOTCON; Oakland, USA). The estimation of the post-absorptive parameters within the Parameter Estimation module of the Simcyp® Simulator was performed with the Maximum Likelihood method.[32] The prediction accuracy of the simulated plasma profiles was evaluated with the average fold error (AFE) and absolute average fold error (AAFE) (Equations 1 and 2),

$$AFE = 10^{\frac{1}{n}\sum \log\left(\frac{pred_t}{obs_t}\right)} \quad (1)$$

$$AAFE = 10^{\frac{1}{n}\sum \left|\log\left(\frac{pred_t}{obs_t}\right)\right|} \quad (2)$$

where n is the number of time points at which the concentration was determined and $pred_t$, obs_t are the predicted and observed concentrations at a given time point t, respectively. An AFE greater or smaller than one indicates an overestimation or underestimation of the observed data, respectively, whereas $AAFE$ is a measure of the absolute error from the true value. An $AAFE \leq 2$ can be considered as a successful prediction.[33,34]

Statistical analysis (including calculation of 95% CIs) was performed with Simcyp® (V17.1; Certara, Sheffield, UK).

3. Results

3.1 In vitro studies

3.1.1 Solubility experiments

Mean solubility values (± SD) of crystalline etravirine at 24 h in Level I and Level III FaSSGF, Level I and Level II FaSSIF V1, FaSSIF V2, FaSSIF V3, FeSSIF V1, FeSSIF V2 and FeSSGF are presented in Table 2, together with the pH values recorded at the end of the solubility experiment (pH_{final}), as well as solubility values in pooled human aspirates that have been reported in literature.

The solubility of crystalline etravirine was below LOQ, i.e. 0.05 µg/mL, in all Level I biorelevant media measured. It is interesting to note that the solubility of crystalline etravirine in Level III FaSSGF was also

below the LOQ, despite the fact that etravirine is a weak base and thus higher solubility values are expected in media with acidic pH. These data are in line with those of Bevernage et al., who reported extremely low solubility values in Level II FaSSGF (approximately 0.009 µg/mL).[10]

By contrast, the solubility values of crystalline etravirine in Level II biorelevant media simulating the gastric and intestinal fluids in fasted and fed states were measurable and were dependent on the amount and type of surfactants used in the respective medium. In particular, comparison of solubility between Level I and II media reveals the role of naturally occurring surfactants in the solubility of etravirine. These data are in line with those of Bevernage et al., who reported similar values in Level II FaSSIF V1 and Level II FeSSIF V1 (approximately 1 µg/mL and 6.2 µg/mL, respectively).[10,18]

Bevernage et al. also performed solubility measurements of crystalline etravirine in pooled human aspirates. These researchers aspirated gastric and intestinal fluids from healthy volunteers in the fasted state (FaHGF, n=4 and FaHIF, n=5, respectively), as well as in the fed state after administration of Ensure Plus® (29% fat content, FeHIF), or Scandishake Mix® (46% fat content, "Fat enriched"-FeHIF).[10,18] The solubility of etravirine observed in FaHIF (with a total bile salt concentration of 5.4 ± 0.058 mM) was approximately 1.5 µg/mL, whereas in FeHIF (with a total bile salt concentration of 10.4 ± 1.2 mM) it was around 4 µg/mL and in "Fat enriched"-FeHIF (with a total bile salt concentration of 12.7 ± 0.2 mM) it was 8.3 µg/mL. These results underline the large effect of native surfactants on the solubilization of etravirine.

Table 2: Mean solubility (± SD) at 24 h of crystalline etravirine in various biorelevant media used in the present study, pH recorded at the end of the solubility experiment (pH_{final}) and solubility of crystalline etravirine in human aspirates reported in literature.

Medium	Solubility ± SD (µg/mL)	pH_{final}
Biorelevant media		
Level I FaSSGF	<LOQ	1.6
Level III FaSSGF	<LOQ	1.6
Level I FaSSIF V1	<LOQ	6.5
Level II FaSSIF V1	0.70 ± 0.02	6.5
Level I FaSSIF V2	<LOQ	6.5

Level II FaSSIF V2	0.24 ± 0.02	6.5
Level I FaSSIF V3	<LOQ	6.5
Level II FaSSIF V3	0.11 ± 0.03	6.7
Level II FeSSGF	3.66 ± 0.09	5.0
Level I FeSSIF V1	<LOQ	5.0
Level II FeSSIF V1	3.25 ± 0.13	5.0
Level I FeSSIF V2	<LOQ	5.9
Level II FeSSIF V2	3.47 ± 0.13	5.9
Human aspirates[10,18]		
FaHGF	0.06	1.6
FaHIF	1.5	6.7
FeHIF	4.05	6.2
Fat enriched-FeHIF	8.3	6.0

317

318 3.1.2 Dissolution experiments

319 Dissolution experiments were performed on Intelence® tablets at both dose strengths in biorelevant
320 media simulating the contents of the fasted stomach (Level III FaSSGF), fasted upper small intestine (Level
321 II FaSSIF V1, FaSSIF V2 and FaSSIF V3), fed stomach (Level II FeSSGF) and fed upper small intestine (Level
322 II FeSSIF V1 and FeSSIF V2).[15] The mean concentration (± SD) of dissolved etravirine with time during the
323 first 4 h of dissolution in these experiments are presented in Figure 1-3.
324 As observed in these figures, dissolution at both doses is fast, incomplete and reaches a maximum value
325 of dissolved etravirine concentration within 15-30 minutes. The dissolution results in biorelevant media
326 simulating the fed vs. fasted state are clearly in agreement with the large food effect (approximately 50%)
327 observed *in vivo* for Intelence® tablets.

328 Once the maximum value is reached, the concentration of dissolved drug decreases to the 24 h value,
329 which is similar for the 100 mg and 200 mg tablets. The time to reach this 24 h value is dependent on the
330 type of biorelevant medium used for the dissolution experiment and the dose / maximum dissolved
331 concentration of etravirine achieved. The 24 h concentrations in the dissolution experiments with the

formulated drug, as well as their ratios to the 24 h solubility value of crystalline etravirine in the respective media, are presented in Table 3. When the 24 h value from the dissolution experiment with the formulated drug is compared with the 24 h solubility value for the crystalline API, it is observed that the concentration of etravirine in the tablet dissolution experiment remains supersaturated over the entire duration of the experiment. DSC experiments conducted with the solid collected at the end of the dissolution experiments revealed the absence of any crystalline drug. Taken together with the concentrations achieved in dissolution of the Intelence® tablets, this result suggests that the solubility of the amorphous form is substantially higher than that of the crystalline form.

When comparing the ratios of the maximum concentrations reached after dissolution of the 200 mg and 100 mg Intelence® tablets in the various versions of biorelevant media, it is interesting to note that the higher ratios (greater than 2) are observed in the media which also contain other components (e.g. glyceryl monooleate in Level II FeSSIF V2) rather than just sodium taurocholate (NaTC) and lecithin (e.g. Level II FaSSIF V1 and FeSSIF V1). This observation suggests that etravirine interacts differently with the various biorelevant components, such that addition of additional lipid components like glycerylmonooleate not only increases the amount of etravirine dissolved, but also leads to a longer duration of drug in solution. This observation is also in agreement with the study of Elkhabaz et al., who observed different interactions between the biorelevant components and the amorphous form of ezetimibe.[3]

Table 3: Etravirine mean (±SD) dissolved concentrations resulting after 24 h dissolution experiments of 100 mg and 200 mg Intelence® tablets (formulated drug) in various biorelevant media and ratios to the 24 h solubility value of the crystalline API.

Medium	Mean concentration of drug dissolved (±SD) after 24 h of dissolution (µg/mL)	Ratio (formulated drug dissolved concentration at 24 h / crystalline drug solubility at 24 h)
Level II FaSSIF V1	6.08 ± 0.22	8.7
Level II FaSSIF V2	1.67 ± 0.10	7.0

Level II FaSSIF V3	0.68 ± 0.08	6.2
Level II FeSSGF	29.42 ± 3.19	8.0
Level II FeSSIF V1	23.87 ± 0.26	7.3
Level II FeSSIF V2	13.40 ± 0.84	3.7

353

354 3.1.3 Transfer experiments

355 Transfer experiments were performed to further investigate the potential for supersaturation and
356 precipitation of etravirine. The mean concentration (± SD) of dissolved etravirine with time during the 4
357 h transfer experiments from Level III FaSSGF to Level II FaSSIF V1, Level II FaSSIF V3 or Level II FaSSIF
358 $V1_{concentrated}$ for the 100 mg and 200 mg Intelence® tablets are presented in Figure 4.
359 In accordance with the monophasic dissolution and solubility experiments, there is a pronounced effect
360 of the amount and type of surfactants of the biorelevant medium on the concentration of etravirine
361 generated in the transfer studies. In particular, the maximum concentration dissolved during the transfer
362 experiments are the highest when the drug is transferred to a medium with an initially higher surfactant
363 concentration, i.e. Level II FaSSIF $V1_{concentrated}$ (5.14 mM NaTC) vs. Level II FaSSIF V1 (3 mM NaTC).
364 Furthermore, as previously mentioned, the type of the surfactant seems to play a role in the dissolution
365 of the amorphous etravirine. When etravirine is transferred from the amorphous solid dispersion into
366 Level II FaSSIF V3, which also contains glycocholate and cholesterol, there is a greater ratio between the
367 maximum concentration dissolved from 200 mg tablets vs. 100 mg tablets in comparison to the ratios
368 achieved when the same formulation is transferred to media containing only sodium taurocholate and
369 lecithin i.e. Level II FaSSIF V1 and Level II FaSSIF $V1_{concentrated}$.
370 Comparing the transfer with the dissolution experiments in media simulating the fasted state, the
371 etravirine concentration starts to decrease later in the transfer experiments (after approximately 90-120
372 min) than in the dissolution experiments (after 30 min), and at a slower rate than observed in the single

medium dissolution experiments. Although it would be interesting to know whether similar differences are observed under fed state conditions, there is currently no validated transfer setup for simulating drug transfer from the fed stomach to the fed small intestine (noting that some early attempts have been made).[35] Nonetheless, the similar maximum concentrations of dissolved etravirine achieved in Level II FeSSGF and Level II FeSSIF V1, together with the moderate permeability of etravirine, suggest that precipitation is unlikely to happen in the fed state *in vivo*.

3.2 PBPK model and simulations

3.2.1 Input of *in vitro* derived parameters and effect of possible precipitation on the simulated profiles

When evaluating the results from the *in vitro* experiments of etravirine and implementing them into the PBPK model, the questions that arise are, for example, which "solubility" is appropriate for the formulated drug? Would etravirine really precipitate *in vivo*? If the answer to the latter question is yes, does it precipitate to a crystalline form or does it form amorphous aggregates? Furthermore, if it does precipitate *in vivo* in the fed state, are the precipitation rate constants observed in the monophasic fed state dissolution experiments representative of the *in vivo* precipitation?

In order to account for all possible scenarios and gain a better understanding of the *in vivo* behavior of etravirine, two approaches were followed when implementing the *in vitro* data in the PBPK model: "no precipitation" and "implementation of precipitation". The simulated plasma profiles after oral administration of a 100 mg or 200 mg Intelence® tablet in the fed state vs. the individual observed plasma concentrations (Janssen data on file), as well as the observed mean pharmacokinetic profiles reported in the literature[12,20,21], following both approaches are presented in Figure 5 and 6. The AFE and AAFE for each simulation approach compared to the observed mean pharmacokinetic profiles are presented in Table 4.

As can be observed in Figure 5, Figure 6 and Table 4, the first approach, i.e. “no precipitation”, appears to be more representative of the behavior of etravirine *in vivo*. In particular, the “no precipitation” approach resulted in a good representation of the individual pharmacokinetic data (Janssen data on file, Figure 5A) after the administration of a 100 mg Intelence® tablet in fed state as well as leading to overall good predictions of the mean observed pharmacokinetic profiles reported in the literature[12,20,21] (Figure 5C), with AAFE mostly ≤ 2. By contrast, the second approach (“implementation of precipitation”) led to substantial underprediction of the pharmacokinetics of etravirine (Figures 5B and 5D). For the 200 mg Intelence® tablets an overall trend for underprediction of the pharmacokinetics of etravirine is observed, however, this trend is far greater when the “implementation of precipitation” approach is used (Figure 6). Comparing these simulations, it appears that etravirine does not precipitate to a significant extent when administered in the fed state *in vivo*. This observation, along with the moderate permeability of etravirine (a P_{app} value of 6.5 x10^{-6} cm/sec which is translated to a P_{eff} of approx. 1.1 x10^{-4} cm/sec with Simcyp® Simulator internal calculation), suggests that it is more informative to consider etravirine as a DCS IIb compound[36] rather than as a BCS Class IV compound.

Table 4: Calculated average fold error (AFE) and absolute average fold error (AAFE) for the simulations of observed plasma profiles after oral administration of Intelence® tablets in the fed state.

Dose	100 mg		200 mg		Published clinical data
Metrics	No precipitation	With precipitation	No precipitation	With precipitation	
AFE	1.55	1.11	1.57	0.74	[20]
AAFE	1.56	1.60	1.93	2.31	
AFE	1.53	1.38	-	-	[12]
AAFE	1.53	1.82	-	-	
AFE	1.97	1.78	-	-	[12]
AAFE	2.04	2.34	-	-	
AFE	1.40	1.25	-	-	[21]
AAFE	1.51	1.94	-	-	
AFE	-	-	0.89	0.42	[22]
AAFE	-	-	1.70	3.00	
AFE	-	-	1.99	0.93	[22]

AAFE	-	-	2.80	3.92

411

412 3.2.2 Post-absorptive parameters that could affect etravirine pharmacokinetics

413 The currently developed model was able to successfully predict the reported mean pharmacokinetic
414 profiles of etravirine after administration of a 100 mg Intelence® tablet. However, the model generally
415 underpredicted the mean pharmacokinetic profiles after administration of a 200 mg Intelence® tablet.
416 Furthermore, at both dose strength levels the 95% CIs were not able to cover all of the individual PK
417 profiles. These observations, in combination with the information provided in the Public Assessment
418 Report of Intelence® regarding the non-linear pharmacokinetics of etravirine[9], the large range of
419 apparent volume of distribution applied in pharmacokinetic models that have been reported so far in the
420 literature (i.e. 420-1370 L)[13,26–29], as well as the fact that only around 20% of the etravirine elimination
421 can be explained mechanistically by the enzyme kinetics and only 5-16% of the overall variability in the
422 apparent clearance of etravirine can be explained by the different phenotypes of CYP2C19 (sections 2.3.2
423 and 2.3.3), suggest that various post-absorptive parameters can have an important effect on the
424 pharmacokinetics of etravirine and that these should also be taken into consideration when simulating
425 the *in vivo* behavior of this compound.
426 With regard to plasma protein binding, Nguyen et al.[37] measured the unbound fraction (f_u) of etravirine
427 as well as the total etravirine plasma concentrations of nine HIV-1 infected patients, who had been taking
428 Intelence® 200 mg twice daily for at least 2 weeks (median duration of etravirine use: eight months). It
429 was shown that the unbound fraction of etravirine varied with the total etravirine plasma concentration,
430 with the fraction unbound increasing with increasing etravirine plasma concentration. The non-linearity
431 of protein binding may therefore contribute to the *in vivo* variability of etravirine. Similar non-linearity of
432 plasma protein binding has been associated with a high *in vivo* variability in f_u among subjects for other
433 anti-retrovirals such as indinavir, saquinavir, atazanavir, darunavir and lopinavir.[38–42]

Assuming a concentration dependency of both f_u and V_d, it is an oversimplification to represent the fraction unbound with a single f_u value and the apparent volume of distribution of etravirine with a single V_d value at all time points and all volunteers, at both dose levels. Furthermore, if f_u and V_d are changing with concentration, clearance will also be changing with time. These concentration-dependent effects are challenging to model, especially since residual clearance is typically set at a fixed value. In simulations performed in the current study, the f_u was set at 0.01, as published in the Public Assessment Report[9] and as used in previously published pop-PK studies e.g. by Molto et al.[25]

In the Simcyp® Simulator V17, the user has the opportunity to simulate such events of concentration-dependent f_u only when a minimal PBPK (mPBPK) model is applied. In an mPBPK model, the user can input the relationship between the drug plasma concentration and the fraction unbound in plasma and then simulate the continuously changing f_u with or without a simultaneous, concentration dependent change in the apparent volume of distribution. For investigational purposes, an mPBPK model was built to explore the effect of a concentration dependent f_u and/or V_d on the pharmacokinetics of etravirine and explain part of the observed high pharmacokinetic variability, noting that in these models all tissues apart from the liver and the portal vein are lumped to a peripheral compartment (Single Adjusting Compartment, SAC), analogous to a classic PK two-compartment distribution model and thus cannot provide any further insight on the distribution/ elimination mechanisms of etravirine. Following a "middle-out" strategy, the post-absorptive parameters associated with the SAC i.e. Q_{SAC} (inter-compartment clearance) (5.70 L/h) and V_{SAC} (apparent volume associated with the SAC) (2.56 L/kg), and additional clearance through other pathways (other than the "Enzyme Kinetic" parameters described in section 2.3.3 and Table 1) (450 and 100 µL/min/mg protein for the 100 mg and 200 mg dose, respectively) were estimated using the Parameter Estimation (PE) Tool by simultaneously fitting of the available pharmacokinetic profiles. The linear relationship between plasma concentration and etravirine plasma f_u was derived from the study of Nuygen et al.[37] It should be noted that the Nuygen study was performed

458 in HIV-positive volunteers who were concomitantly receiving other medication, including emtricitabine
459 (89%), tenofovir (78%), darunavir/ritonavir (78%), raltegravir (56%), enfuvirtide (33%), maraviroc (22%),
460 didanosine (11%) and lamivudine (11%). According to the literature, there are no clinically significant
461 interactions with emtricitabine, tenofovir and raltegravir,[24] and while boosted darunavir decreases the
462 concentrations of etravirine, no dose adjustment is required.[24] No analogous studies are available for
463 healthy volunteers. For the absorption part of the model, the "no precipitation" approach was followed.

464 The simulated plasma profiles after oral administration of a 100 mg or 200 mg Intelence® tablet in the
465 fed state vs. the individual observed plasma concentrations (Janssen data on file) following the minimal
466 PBPK concentration dependent f_u and concentration dependent f_u and V_d strategy, are presented in
467 Figures 7 and 8. As can be observed in Figure 7 and Figure 8, this approach was able to capture the overall
468 *in vivo* variability of the pharmacokinetics of etravirine within the 95% CIs, as well as the plasma
469 concentrations after administration of a 200 mg Intelence® tablet in fed state, more closely than the
470 simulations applying fixed values for f_u and V_d. The results suggest that the f_u likely plays a key role in the
471 pharmacokinetics of etravirine, especially when considering that etravirine binds to α1-acid glycoprotein,
472 for the expression of which high inter-subject variability is observed. However, there are still many
473 question marks around the role of f_u in etravirine's pharmacokinetic behavior and more *in vitro* data
474 would assist in improving the quality of the model and confirming the assumption of a concentration
475 dependent f_u.

476

477

4. Discussion

Bio-enabling formulations have been proven to be a viable solution to overcome the difficult properties, e.g. poor aqueous solubility, associated with various APIs in current development pipelines and to thus facilitate access to innovative medicines. However, there is still considerable lack of understanding regarding the *in vitro* characterization and *in vivo* behavior of these formulations, as well as the mechanisms and extent to which they can improve bioavailability. For example, the *in vitro* characterization of ASDs can be quite complex because of their supersaturation and precipitation behavior, which may be dependent on interactions between the amorphous API and the various biorelevant components.[2,3,43] To date, there has been limited application of PBPK / absorption models in predicting the *in vivo* performance of ASDs due to the complex *in vitro* and *in vivo* dissolution process.[44–46] However, some early attempts have already been published and more, relevant studies are needed to advance our understanding in this field.[44–46] As demonstrated in the current study, the use of biorelevant *in vitro* tools in combination with modeling and simulation techniques provides a way forward to better understand the *in vivo* performance of such formulations.

Since dissolution rate is proportional to C_s-C_t, where C_s is the solubility at particle surface in the respective medium and C_t the concentration of drug in the bulk solution at time t, for bio-enabling formulations it is of great importance to input an appropriate “solubility” value for the formulated drug in order to achieve successful simulation of the dissolution experiment. For etravirine, solubility and dissolution experiments conducted in biorelevant media demonstrated the large effect of naturally occurring surfactants on solubility and consequently the large food effect which is observed *in vivo* for etravirine. Further, comparison of the 24 h solubility of crystalline etravirine with the 24 h concentration achieved in the dissolution vessel during the dissolution experiments of Intelence® tablets in biorelevant media revealed that etravirine remains supersaturated over the entire course of dissolution when presented as an amorphous solid dispersion. Likewise, comparison of simulation results using alternate approaches,

i.e. “no precipitation” and “implementation of precipitation”, led to the conclusion that etravirine does not precipitate *in vivo* when administered in the fed state. For etravirine, it was reasoned that if no precipitation was observed in a transfer experiment conducted under fasted state conditions, it would be even less likely to precipitate in the fed state, where the solubility differential for a weak base is lower than in the fasted state (assuming the fasted state gastric pH is low). This is further supported by the similar maximum concentration of dissolved etravirine achieved in the media simulating the fed stomach and fed upper small intestine. Nevertheless, a standardized model setup which can simulate the transfer of the drug from the fed stomach to the fed upper small intestine would be beneficial to understanding the *in vivo* performance of complex bio-enabling formulations in the fed state.

Lack of precipitation *in vivo* has also been hypothesized in the literature for several other basic compounds. Mitra et al. attempted to predict the *in vivo* performance of the ASDs of three basic compounds (two BCS Class II and one BCS Class IV) by combining *in vitro* data with PBPK modeling.[44] In all cases, there was no need to invoke precipitation in the created PBPK absorption models to achieve successful simulations of the *in vivo* plasma profiles. The same conclusion was reached by Emami-Riedmaier et al. who combined biorelevant *in vitro* data with PBPK modeling to predict the *in vivo* performance of the ASD of the BCS Class IV venetoclax.[46] Similar results have also been observed by Wilson et al. for the ASD of enzalutamide in rats.[2] The authors opined that the absence of crystallization of enzalutamide along with the interplay of *in vivo* permeation, diffusion and dissolution creates a continuous sink for an amorphous compound and thus facilitates its *in vivo* absorption.[2] From the aforementioned studies published in literature, as well as from the present study, it is very interesting to note that the maximum dissolved concentration achieved in the dissolution vessel in the respective biorelevant media was used in every case to represent the *in vivo* solubility of the API administered as the respective ASD.

By contrast, the use of the *in vitro* solubility of the crystalline API to represent *in vivo* solubility can result in a large underprediction of absorption[46], as shown previously, for example, by Litou et al. for the bio-enabling formulation of aprepitant[4].

Last but not least, as observed for etravirine pharmacokinetics, post-absorptive processes can also have a significant effect on the plasma profiles of many APIs and these should not be ignored. Rather, these parameters should also be investigated in order to be able to understand the overall *in vivo* behavior of these APIs and draw robust conclusions about the extent to which formulation options can be used to influence the API's pharmacokinetics. Using modelling and simulation, it was feasible to investigate the scenario of a concentration dependent f_u and V_d for etravirine. By invoking a concentration dependent relationship instead of single values for these parameters, it was possible to better represent the variability of etravirine pharmacokinetics observed *in vivo*. As no data for the concentration dependency of f_u and V_d was available in healthy volunteers, it was necessary for investigational purposes to apply data from HIV-positive volunteers to the healthy population. Although the results may not be fully representative, they do suggest that these two post-absorptive parameters contribute more to the variability in the pharmacokinetics of etravirine than metabolic variations, and should thus be taken into account in future simulations of etravirine and other APIs with proven concentration-dependent plasma binding and volume of distribution.

Comparing the influence of pre- and post-absorptive parameters on the pharmacokinetic profile of etravirine after oral administration of the commercial ASD formulation, it appears that the key factor on the pre-absorption side is the maximum achievable supersaturation concentration attainable with the ASD, which is the driving force for increasing the extent of absorption, while on the post-absorptive side, the concentration dependency of plasma binding and volume of distribution are the key contributors to the extensive variability in plasma profiles.

5. Conclusions

Despite the recent work and research around bio-enabling formulations, there is still lack of fundamental understanding with regard to their *in vivo* performance, the changes that may occur in the physicochemical properties of the API (for example formation of amorphous drug, nano-crystals, interactions with polymers, which act as precipitation inhibitors etc.) and how this information can be implemented into *in silico* PBPK models. In this study, the *in vivo* performance of the etravirine "enhanced" formulation (Intelence® tablets) in healthy volunteers in the fed state, was successfully predicted by coupling *in vitro* data, acquired with biorelevant *in vitro* tools, with a commercial PBPK modeling platform (the Simcyp Simulator). This case example demonstrated the potential application and importance of absorption modeling in rational formulation design and in strengthening biopharmaceutics knowledge around amorphous solid dispersions. Furthermore, this study also demonstrated the importance of evaluating the effect of both pre- and post-absorptive parameters. Following a similar approach can help identify the main parameters which affect the pharmacokinetic behavior of poorly soluble APIs formulated as bio-enabling formulations and thus allow for robust clinical outcome predictions.

Acknowledgments

This work was supported by the European Union's Horizon 2020 Research and Innovation Programme under grant agreement No 674909 (PEARRL), www.pearrl.eu.

The authors would like to thank Ms. Manuela Thurn for her valuable help with the DSC measurements.

References

1. Buckley ST *et al.* Biopharmaceutical classification of poorly soluble drugs with respect to "enabling formulations". *Eur J Pharm Sci* 2013; 50(1): 8–16. doi:10.1016/j.ejps.2013.04.002.

2. Wilson V *et al.* Relationship between amorphous solid dispersion in vivo absorption and in vitro dissolution: phase behavior during dissolution, speciation, and membrane mass transport. *J Control Release* 2018; 292: 172–182. doi:10.1016/j.jconrel.2018.11.003.

3. Elkhabaz A *et al.* Variation in Supersaturation and Phase Behavior of Ezetimibe Amorphous Solid Dispersions upon Dissolution in Different Biorelevant Media. *Mol Pharm* 2018; 15(1): 193–206. doi:10.1021/acs.molpharmaceut.7b00814.

4. Litou C *et al.* Combining biorelevant in vitro and in silico tools to simulate and better understand the in vivo performance of a nano-sized formulation of aprepitant in the fasted and fed states. *Eur J Pharm Sci* 2019; 138: 105031. doi:10.1016/j.ejps.2019.105031.

5. Deeks ED, Keating GM. Etravirine. 2008; 68(16): 2357–2372.

6. EMA. Intelence: Summary of Product Characteristics. Available at: https://www.ema.europa.eu/en/documents/product-information/intelence-epar-product-information_en.pdf. Accessed July 24, 2019.

7. FDA. Intelence Drug Approval Package. Available at: https://www.accessdata.fda.gov/drugsatfda_docs/nda/2008/022187TOC.cfm. Accessed July 24, 2019.

8. Weuts I *et al.* Physicochemical properties of the amorphous drug, cast films, and spray dried powders to predict formulation probability of success for solid dispersions: Etravirine. *J Pharm Sci* 2011; 100(1): 260–274. doi:10.1002/jps.22242.

9. EMEA (European Medicines Agency). INTELENCE: Etravirine CHMP Assessment Report. *43952* 2008: 1–52. Available at: http://www.ema.europa.eu/docs/en_GB/document_library/EPAR_-_Public_assessment_report/human/000900/WC500034183.pdf.

10. Bevernage J *et al.* Supersaturation in human gastric fluids. *Eur J Pharm Biopharm* 2012; 81(1): 184–189. doi:10.1016/j.ejpb.2012.01.017.

11. Moltó J. Physiologically based pharmacokinetic model to predict drug-drug interaction in patients receiving antiretroviral and antineoplastic therapies. In: *16th HIVHEPPK*. Alexandria, VA, 2015.

12. Schöller-Gyüre M *et al.* Effects of different meal compositions and fasted state on the oral bioavailability of etravirine. *Pharmacotherapy* 2008; 28(10): 1215–1222. doi:10.1592/phco.28.10.1215.

13. Rajoli RKR *et al.* Physiologically Based Pharmacokinetic Modelling to Inform Development of Intramuscular Long-Acting Nanoformulations for HIV. *Clin Pharmacokinet* 2015; 54(6): 639–650. doi:10.1007/s40262-014-0227-1.

14. Bevernage J *et al.* Drug Supersaturation in Simulated Human Intestinal Fluids Representing Different Nutritional States. *J Pharm Sci* 2010; 99(11): 4525–4534.

15. Markopoulos C *et al.* In-vitro simulation of luminal conditions for evaluation of performance of oral drug products: Choosing the appropriate test media. *Eur J Pharm Biopharm* 2015; 93: 173–

182. doi:10.1016/j.ejpb.2015.03.009.

16. Fuchs A *et al.* Advances in the design of fasted state simulating intestinal fluids: FaSSIF-V3. *Eur J Pharm Biopharm* 2015; 94: 229–240. doi:10.1016/j.ejpb.2015.05.015.

17. Andreas CJ *et al.* In vitro biorelevant models for evaluating modified release mesalamine products to forecast the effect of formulation and meal intake on drug release. *Eur J Pharm Biopharm* 2015; 97: 39–50. doi:10.1016/j.ejpb.2015.09.002.

18. Bevernage J *et al.* Drug Supersaturation in Simulated Human Intestinal Fluids Representing Different Nutritional States. *J Pharm Sci* 2010; 99(11): 4525–4534. doi:10.1002/jps.22154.

19. Berlin M *et al.* Prediction of oral absorption of cinnarizine – A highly supersaturating poorly soluble weak base with borderline permeability. *Eur J Pharm Biopharm* 2014; 88(3): 795–806. doi:10.1016/j.ejpb.2014.08.011.

20. Kakuda TN *et al.* Single-dose pharmacokinetics of pediatric and adult formulations of etravirine and swallowability of the 200-mg tablet: results from three Phase 1 studies. *Int J Clin Pharmacol Ther* 2013; 51(9): 725–737. doi:10.5414/CP201770.

21. Schöller-Gyüre M *et al.* A pharmacokinetic study of etravirine (TMC125) co-administered with ranitidine and omeprazole in HIV-negative volunteers. *Br J Clin Pharmacol* 2008; 66(4): 508–516. doi:10.1111/j.1365-2125.2008.03214.x.

22. Schöller-Gyüre M *et al.* Effects of hepatic impairment on the steady-state pharmacokinetics of etravirine 200 mg BID: An open-label, multiple-dose, controlled Phase I study in adults. *Clin Ther* 2010; 32(2): 328–337. doi:10.1016/j.clinthera.2010.02.013.

23. Yanakakis LJ, Bumpus NN. Biotransformation of the antiretroviral drug etravirine: Metabolite identification, reaction phenotyping, and characterization of autoinduction of cytochrome P450-dependent metabolism. *Drug Metab Dispos* 2012; 40(4): 803–814. doi:10.1124/dmd.111.044404.

24. Brayfield A. *Martindale: The Complete Drug Reference, Volume A*., 37th ed. (Sweetman SC, ed.). London, UK: Pharmaceutical Press, 2011.

25. Moltó J *et al.* Use of a physiologically based pharmacokinetic model to simulate drug–drug interactions between antineoplastic and antiretroviral drugs. *J Antimicrob Chemother* 2016; (December 2016): dkw485. doi:10.1093/jac/dkw485.

26. Green B *et al.* Evaluation of Concomitant Antiretrovirals and CYP2C9/CYP2C19 Polymorphisms on the Pharmacokinetics of Etravirine. *Clin Pharmacokinet* 2017; 56(5): 525–536. doi:10.1007/s40262-016-0454-8.

27. Lubomirov R *et al.* Pharmacogenetics-based population pharmacokinetic analysis of etravirine in HIV-1 infected individuals. *Pharmacogenet Genomics* 2013; 23(1): 9–18. doi:10.1097/FPC.0b013e32835ade82.

28. Kakuda TN *et al.* Pharmacokinetics and Pharmacodynamics of the Non-Nucleoside Reverse-Transcriptase Inhibitor Etravirine in Treatment-Experienced HIV-1-Infected Patients. *Clin Pharmacol Ther* 2010; 88(5): 695–703. doi:10.1038/clpt.2010.181.

29. Siccardi M *et al.* Prediction of Etravirine Pharmacogenetics using a Physiologically Based Pharmacokinetic approach. *20th Conf Retroviruses Opportunistic Infect Atlanta, USA* 2013.

30. Jamei M *et al.* Population-based mechanistic prediction of oral drug absorption. *AAPS J* 2009; 11(2): 225–37. doi:10.1208/s12248-009-9099-y.

31. S. Darwich A *et al.* Interplay of Metabolism and Transport in Determining Oral Drug Absorption and Gut Wall Metabolism: A Simulation Assessment Using the "Advanced Dissolution, Absorption, Metabolism (ADAM)" Model. *Curr Drug Metab* 2010; 11(9): 716–729. doi:10.2174/138920010794328913.

32. Tsamandouras N *et al.* Combining the "bottom up" and "top down" approaches in pharmacokinetic modelling: Fitting PBPK models to observed clinical data. *Br J Clin Pharmacol* 2015; 79(1): 48–55. doi:10.1111/bcp.12234.

33. Obach RS *et al.* The prediction of human pharmacokinetic parameters from preclinical and in vitro metabolism data. *J Pharmacol Exp Ther* 1997; 283(1): 46–58. Available at: http://www.ncbi.nlm.nih.gov/pubmed/9336307. Accessed February 9, 2018.

34. Poulin P, Theil F-P. Development of a novel method for predicting human volume of distribution at steady-state of basic drugs and comparative assessment with existing methods. *J Pharm Sci* 2009; 98(12): 4941–4961. doi:10.1002/JPS.21759.

35. Pentafragka C *et al.* The impact of food intake on the luminal environment and performance of oral drug products with a view to *in vitro* and *in silico* simulations: a PEARRL review. *J Pharm Pharmacol* 2019; 71(4): 557–580. doi:10.1111/jphp.12999.

36. Butler JM, Dressman JB. The Developability Classification System: Application of Biopharmaceutics Concepts to Formulation Development. *J Pharm Sci* 2010; 99(12): 4940–4954. doi:10.1002/jps.22217.

37. Nguyen A *et al.* Etravirine in CSF is highly protein bound. *J Antimicrob Chemother* 2013; 68(5): 1161–1168. doi:10.1093/jac/dks517.

38. Sudhakaran S *et al.* Differential protein binding of indinavir and saquinavir in matched maternal and umbilical cord plasma. *Br J Clin Pharmacol* 2007; 63(3): 315–321. doi:10.1111/j.1365-2125.2006.02766.x.

39. Anderson PL *et al.* Indinavir plasma protein binding in HIV-1-infected adults. *AIDS* 2000; 14(15): 2293–2297. doi:10.1097/00002030-200010200-00010.

40. Bohnert T, Gan LS. Plasma protein binding: From discovery to development. *J Pharm Sci* 2013; 102(9): 2953–2994. doi:10.1002/jps.23614.

41. Delille CA *et al.* Effect of protein binding on unbound atazanavir and darunavir cerebrospinal fluid concentrations. *J Clin Pharmacol* 2014; 54(9): 1063–1071. doi:10.1002/jcph.298.

42. Back; MBHLBSKDP. Lopinavir Protein Binding In Vivo Through the 12-hour Dosing Interval. *Ther Drug Monit* 2004; 26(1): 35–39.

43. Park K. Different phase behaviors of enzalutamide amorphous solid dispersions. *J Control Release* 2018; 292: 277–278. doi:10.1016/j.jconrel.2018.11.021.

44. Mitra A *et al.* Physiologically Based Absorption Modeling for Amorphous Solid Dispersion Formulations. *Mol Pharm* 2016; 13(9): 3206–3215. doi:10.1021/acs.molpharmaceut.6b00424.

45. Purohit HS *et al.* Investigating the Impact of Drug Crystallinity in Amorphous Tacrolimus Capsules on Pharmacokinetics and Bioequivalence Using Discriminatory In Vitro Dissolution Testing and

Physiologically Based Pharmacokinetic Modeling and Simulation. *J Pharm Sci* 2018; 107(5): 1330–1341. doi:10.1016/j.xphs.2017.12.024.

46. Emami Riedmaier A *et al.* Mechanistic Physiologically Based Pharmacokinetic Modeling of the Dissolution and Food Effect of a Biopharmaceutics Classification System IV Compound—The Venetoclax Story. *J Pharm Sci* 2018. doi:10.1016/j.xphs.2017.09.027.

Figure Captions

Figure 1: Mean (±SD) concentration of dissolved etravirine from 100 mg (●) and 200 mg (◆) Intelence® tablets in various media simulating the fasted upper small intestine: A) Level II FaSSIF V1, B) Level II FaSSIF V2 and C) Level II FaSSIF V3. The solid and dotted lines represent the 24 h solubility value of crystalline etravirine and the 24 h value resulting from the dissolution experiments of the formulated drug, respectively.

Figure 2: Mean (±SD) concentration of dissolved etravirine from 100 mg (●) and 200 mg (◆) Intelence® tablets in Level II FeSSGF. The solid and dotted lines represent the 24 h solubility value of crystalline etravirine and the 24 h value resulting from the dissolution experiments of the formulated drug, respectively.

Figure 3: Mean (±SD) concentration of dissolved etravirine from 100 mg (●) and 200 mg (◆) Intelence® tablets in various media simulating the fed upper small intestine: a) Level II FeSSIF V1 and b) Level II FeSSIF V2. The solid and dotted lines represent the 24 h solubility value of crystalline etravirine and the 24 h value resulting from the dissolution experiments of the formulated drug, respectively.

Figure 4: Mean (±SD) concentration of dissolved etravirine from A) 100 mg and B) 200 mg Intelence® tablets in Level II FaSSIF V1 (◆), Level II FaSSIF V3 (■) and Level II FaSSIF $V1_{concentrated}$ (●) after transfer from Level III FaSSGF.

Figure 5: Simulated (thick solid line, population mean; thin dashed lines, 5^{th} and 95^{th} percentile of population) and clinically reported plasma concentrations after administration of a 100 mg Intelence®

718 tablet following: A)/C) the first ("no-precipitation") and B)/D) the second ("implementation of
719 precipitation") approach, in fed state. With circles (●) the individual pharmacokinetic data (Janssen data
720 on file), whereas with x's (×) and diamonds (◆), squares (■) and triangles (▲) the mean pharmacokinetic
721 profiles reported by Kakuda et al.[20] and Schöller-Gyüre et al.[12,21] are presented, respectively.
722
723 **Figure 6**: Simulated (thick solid line, population mean; thin dashed lines, 5th and 95th percentile of
724 population) and clinically reported plasma concentrations after administration of a 200 mg Intelence®
725 tablet following: A)/C) the first ("no-precipitation") and B)/D) the second ("implementation of
726 precipitation") approach, in fed state. With circles (●) the individual pharmacokinetic data (Janssen data
727 on file), whereas with x's (×) and diamonds (◆), squares (■) and triangles (▲) the mean pharmacokinetic
728 profiles reported by Kakuda et al.[20] and Schöller-Gyüre et al.[22] are presented, respectively.
729
730 **Figure 7**: Simulated (thick solid line, population mean; thin solid lines, 5th and 95th percentile of
731 population) and clinically reported plasma concentrations after administration of a 100 mg Intelence®
732 tablet following the minimal PBPK strategy with A) concentration dependent f_u and B) concentration
733 dependent f_u and V_d, in fed state. Circles (●) represent the individual pharmacokinetic data (Janssen data
734 on file).
735
736 **Figure 8**: Simulated (thick solid line, population mean; thin solid lines, 5th and 95th percentile of
737 population) and clinically reported plasma concentrations after administration of a 200 mg Intelence®
738 tablet following the minimal PBPK strategy with A) concentration dependent f_u and B) concentration

739 dependent f_u and V_d, in fed state. Circles (●) represent the individual pharmacokinetic data (Janssen data

740 on file).

741

742

Figure 1

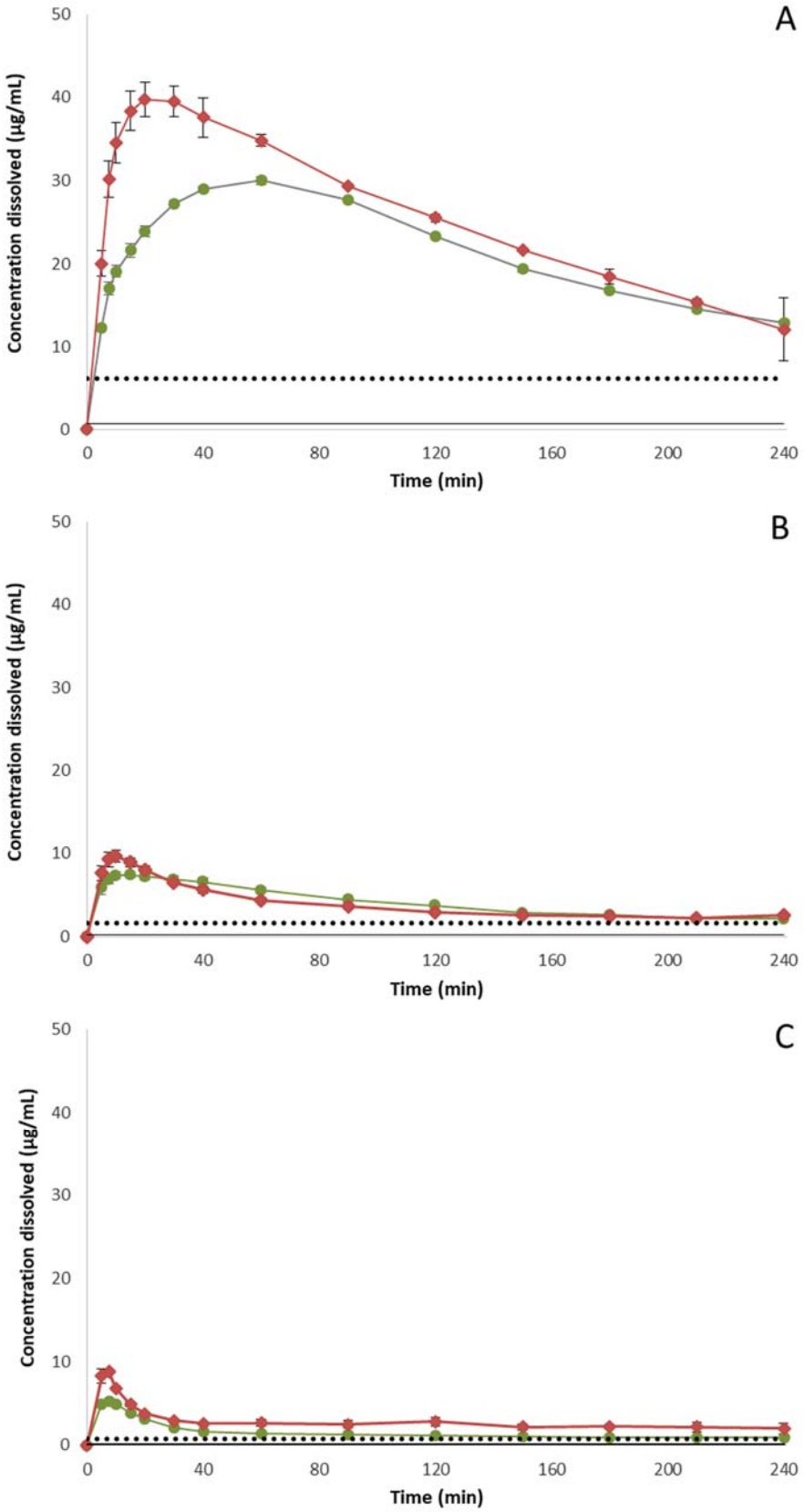

743

744

Figure 2

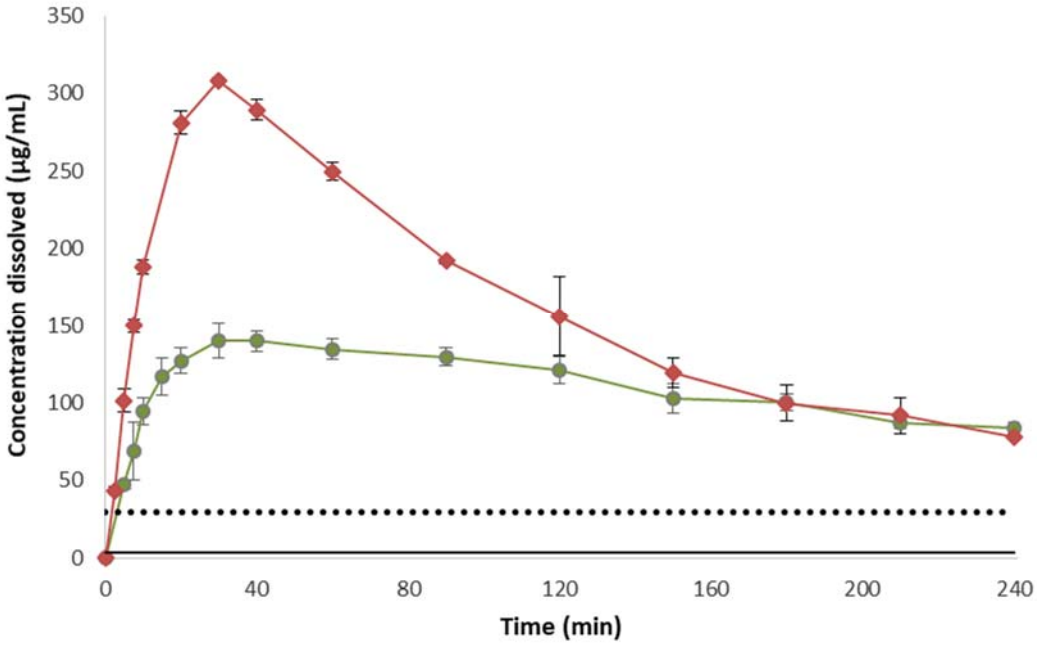

745

746

Figure 3

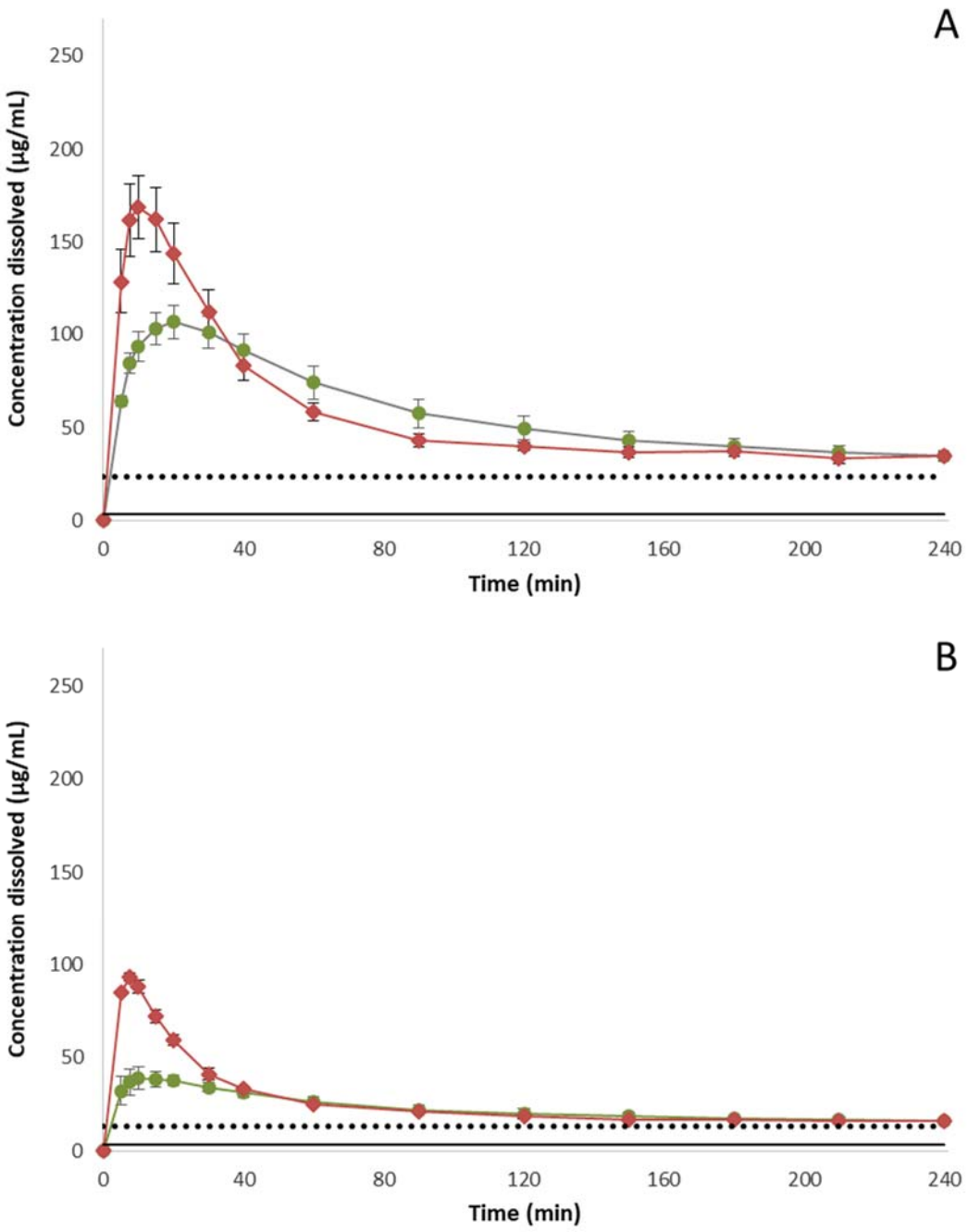

747

748

749

Figure 4

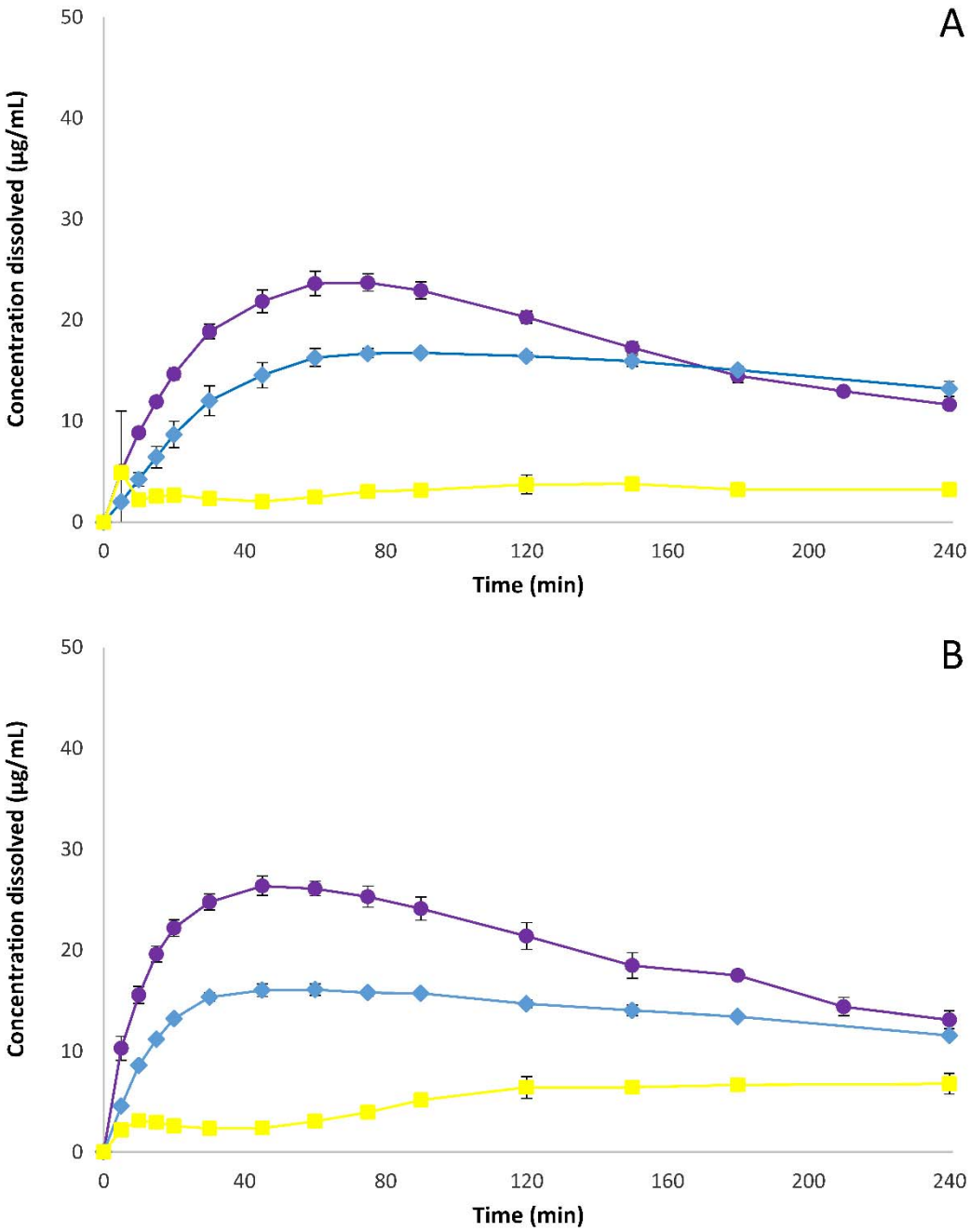

750

Figure 5

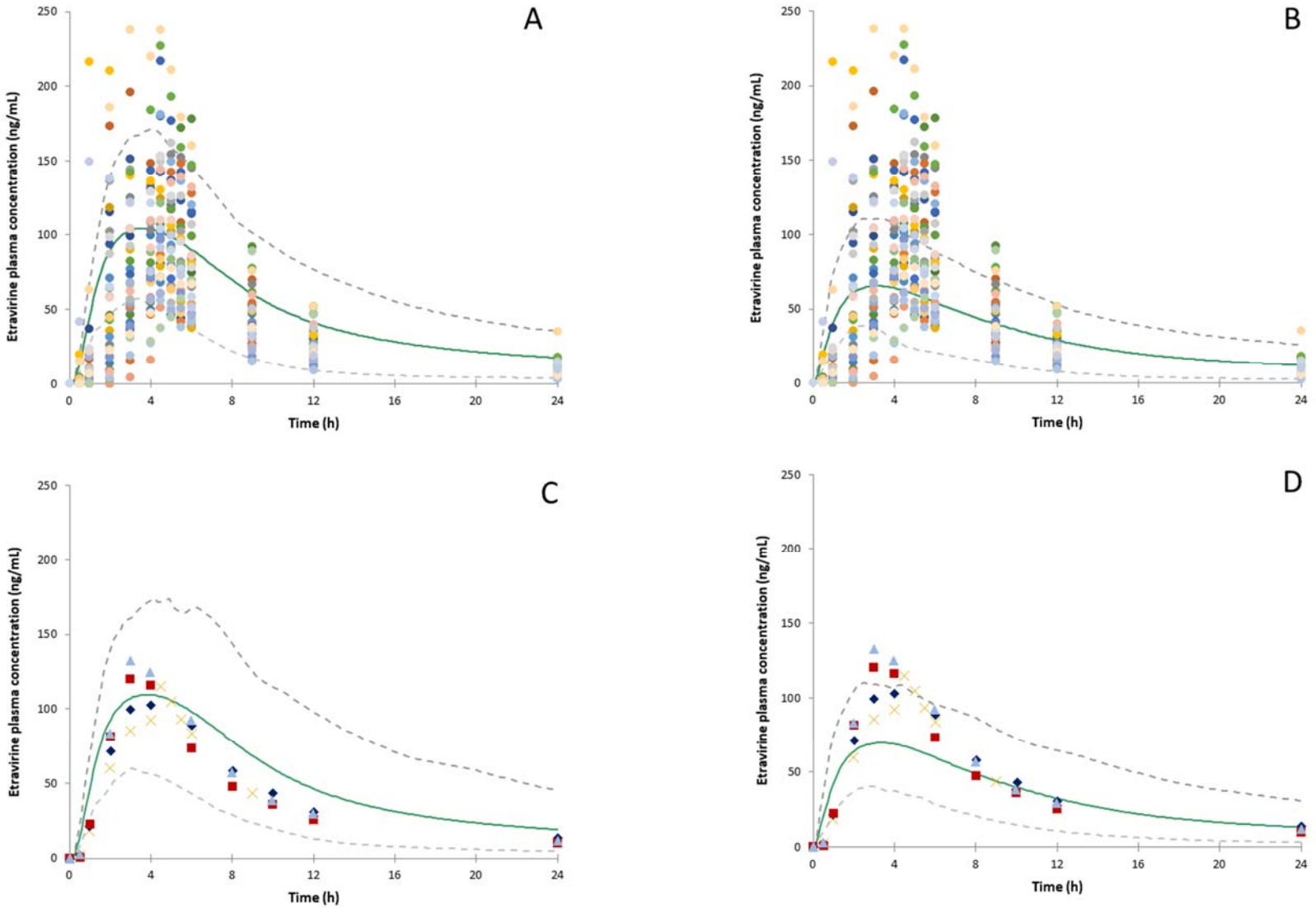
A
B
C
D
Etravirine plasma concentration (ng/mL)
Time (h)
0
50
100
150
200
250
0
4
8
12
16
20
24

753

Figure 6

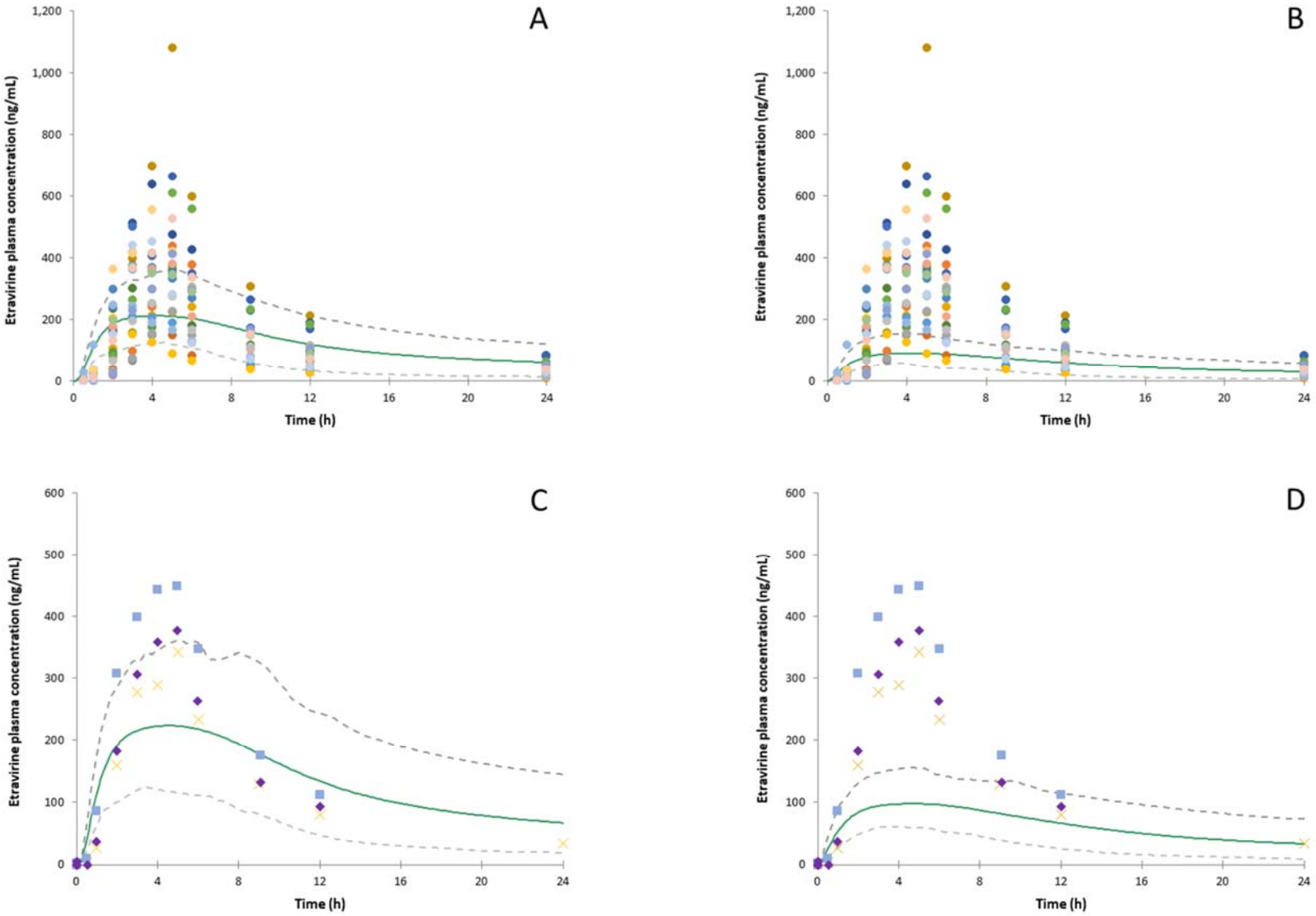

754

755

Figure 7

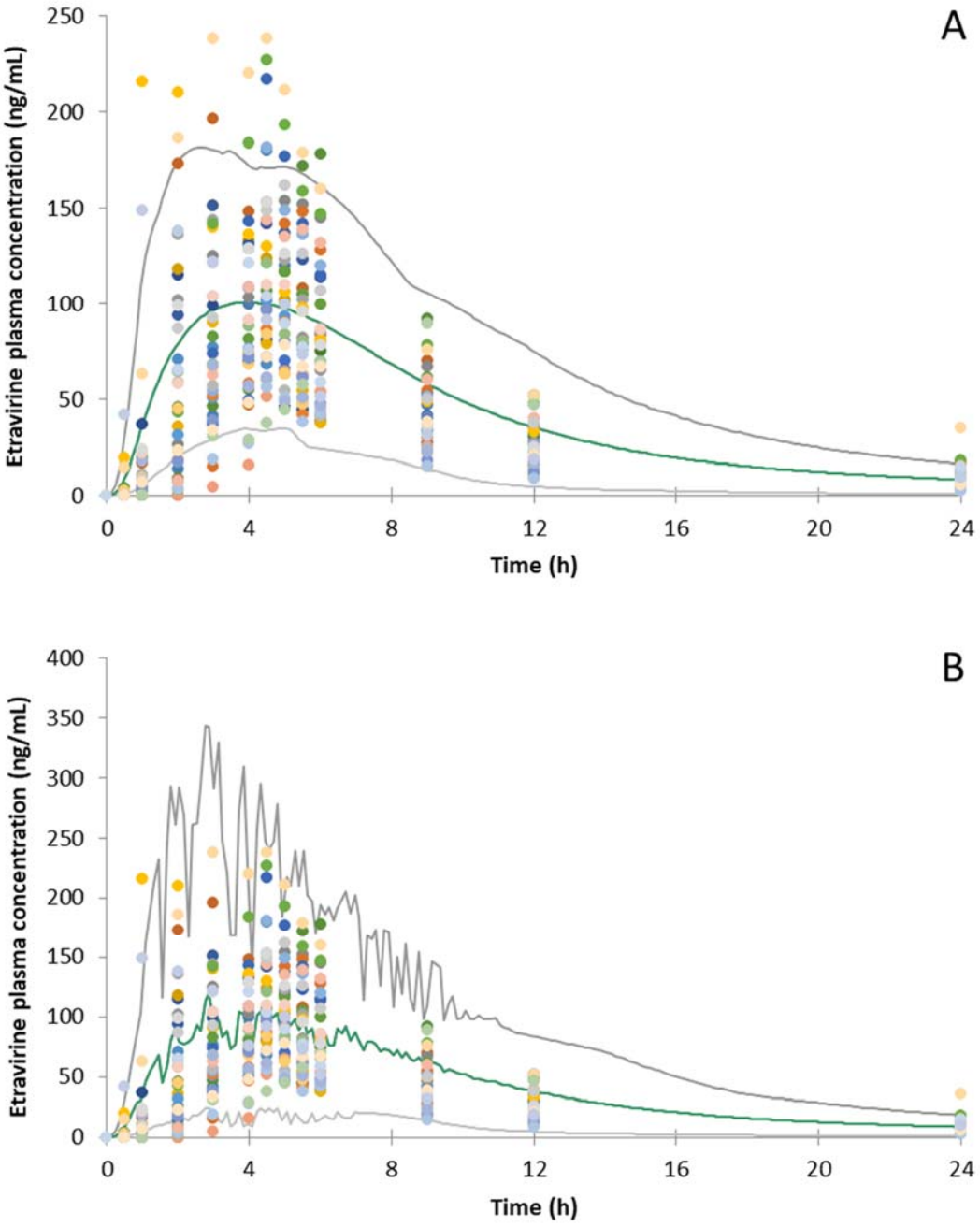

756

757

758

Figure 8

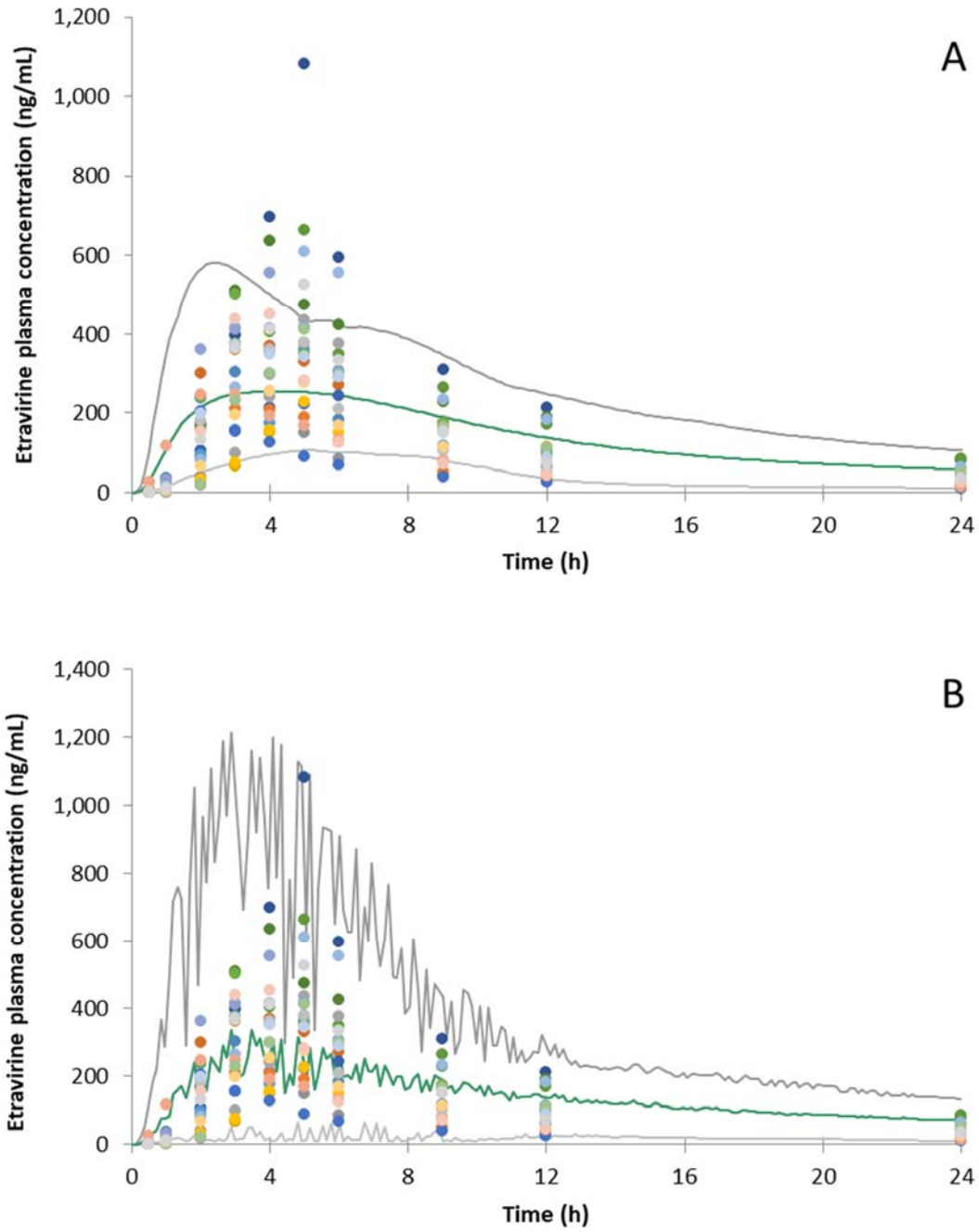

759